12th IMEKO TC4 International Symposium
Electrical Measurements and Instrumentation
September 25–27, 2002, Zagreb, Croatia

METROLOGICALLY IMPROVED DESIGN OF COMBINED CURRENT-VOLTAGE INSTRUMENT TRANSFORMER BY USING FEM-3D

Marija Cundeva, Ljupco Arsov

University "Sts. Cyril & Methodius", Faculty of Electrical Engineering, Skopje, R. Macedonia

Abstract – In the paper a new and original FEM-3D approach to the analysis and design of 20 kV combined current-voltage instrument transformer is given. For the complex study of the electromagnetic field phenomena in the compound configuration with two non-linear magnetic cores of this instrument transformer the finite element method in the three-dimensional domain is used. The FEM-3D derived results will be applied for calculation of the magnetic field distribution in the 3D domain, as well as for the determination of the leakage reactances of the transformer winding. This enables metrologically improved design of the prototype of the transformer, through numerical calculation of the metrological error characteristics of the combined instrument transformer.

Keywords: Instrument transformer, FEM-3D.

1. INTRODUCTION

The instrument transformers as a part of the power measurement systems require high accuracy of transformed voltages and currents, [1]. The 20 kV combined current-voltage instrument transformer (voltage transformation ratio: $20000\ V/\sqrt{3} : 100\ V/\sqrt{3}$ and current transformation ratio: $100\ A : 5\ A$) is a highly non-linear electromagnetic system consisting of two tape-wounded ring magnetic measurement cores (voltage and current transformation core) with mutual magnetic influence which leads to increased voltage, current and phase difference measurement errors [2-4]. The exactness of the derived measurement characteristics depends on the calculation accuracy of the leakage reactances of the instrument transformer windings. The analytical formulas are correct only for constructions with one frame core and cylindrical coaxial windings located on the same column of the core, [4]. For other systems, like the combined instrument transformer with two magnetic cores and complex configuration of the winding system, as shown in Fig. 1, using the field methods is indispensable, [4]. Therefore, the finite element method for 3D magnetic field analysis of the instrument transformer is used, [5].

2. THREE DIMENSIONAL MAGNETIC FIELD MODELLING OF COMBINED INSTRUMENT TRANSFORMER

The magnetic field distribution in the combined current-voltage instrument transformer as a closed and bounded system is described by the system of Maxwell's equations. The magnetic vector potential $\boldsymbol{A}$ as an auxiliary quantity is introduced:

$$\boldsymbol{B} = rot\boldsymbol{A} \tag{1}$$

$$div\boldsymbol{B} = 0 \tag{2}$$

By the Poison's non-linear differential equation in its developed form (3) the magnetic field distribution is expressed as follows:

$$\frac{\partial}{\partial x}\left(\nu(\boldsymbol{B})\frac{\partial \boldsymbol{A}}{\partial x}\right)+\frac{\partial}{\partial y}\left(\nu(\boldsymbol{B})\frac{\partial \boldsymbol{A}}{\partial y}\right)+ +\frac{\partial}{\partial z}\left(\nu(\boldsymbol{B})\frac{\partial \boldsymbol{A}}{\partial z}\right)=-\boldsymbol{j}(x,y,z) \tag{3}$$

where is $\boldsymbol{A}$ the magnetic vector potential, $\boldsymbol{B}$ the magnetic flux density, $\boldsymbol{\nu}$ the magnetic reluctivity and $\boldsymbol{j}(x, y, z)$ the volume current density. The combined instrument transformer is a heterogeneous and non-linear domain with two electromagnetically coupled measuring cores and prescribed boundary conditions. Therefore, the variable coefficients type equation (3) can be solved by numerical methods, only [5].

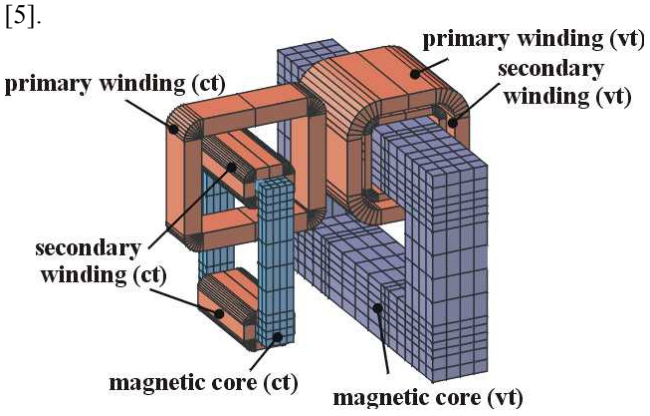

Fig. 1. Active parts of the electromagnetic system of combined instrument transformer
ct - current transformer elements;
vt - voltage transformer elements

The magnetic field analysis is made by a new, original algorithm and universal program package FEM-3D, developed at the Faculty of Electrical Engineering-Skopje, [5]. The program package consists of five main modules shown in Fig. 2:

G1 - automatic mesh generator, input of material properties and current sources;
G2 - mesh and flux plot;
G3 - input definition of boundary conditions;
G4 - magnetic field calculator;
G5 - electromagnetic characteristics calculator.

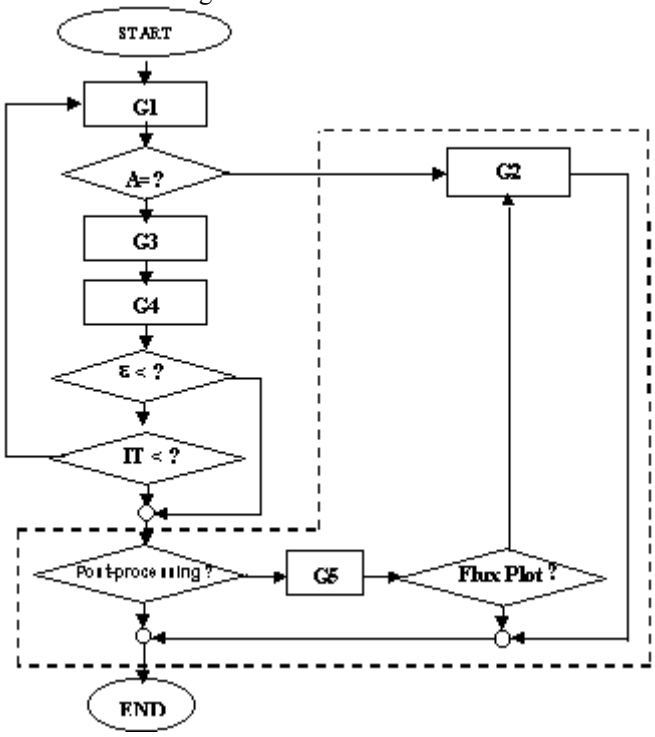

Fig. 2. Flow chart of the FEM-3D program package

For appropriate geometrical and mathematical modelling of the compound configuration of the transformer, the three-dimensional domain is divided into 19 layers along the z-axis: primary and secondary windings (eight layers), two magnetic cores (four layers), isolation areas (seven layers). For the purposes of the 3D finite element method calculations, the magnetic anisotropy and the different reluctivities along the co-ordinate axes are taken into consideration, [5]. The lamination of the magnetic cores are also taken into account. The mesh of finite elements is particularly adjusted to convenient modelling of the primary and secondary windings and the magnetic cores of both parts of the instrument transformer (current and voltage transformation) as shown in Fig. 1. The input primary voltage (for the voltage transformer) as well as the input primary current (for the current transformer) are changed from 0 to 120 % of their nominal values, with step of 20% of the nominal values. The complex study is made for all different combinations of input voltage and current values at constant loads of the both transformation cores (S_{nu}=50 VA for the voltage transformation and S_{ni}=15 VA for the current transformation and $cos\varphi$=0,8). After the non-linear iterative calculation of the magnetic vector potential in the whole investigated 3D-domain is accomplished, the magnetic field distribution is derived. The magnetic flux density is numerically estimated at different parts of the two magnetic cores. The flux plots in the middle cross-sections of the two magnetic cores are shown in Fig. 3 and Fig. 4.

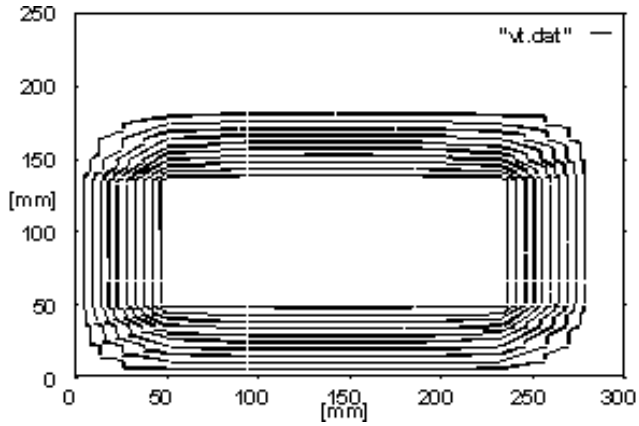

Fig. 3. Flux plot in the middle cross-section of the voltage transformation measuring core (layer 5)

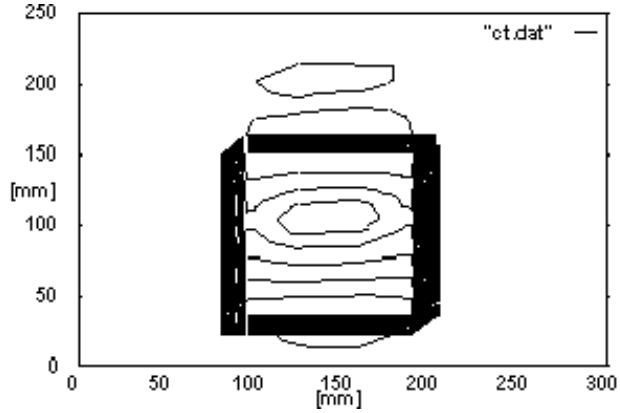

Fig. 4. Flux plot in the middle cross-section of the current transformation measuring core (layer 15)

Numerical calculation of the fluxes Ψ is carried out on the basis of the field theory by using the numerical integration in the FEM-3D.

$$\Psi = \iint \boldsymbol{B} \cdot \boldsymbol{ndS} = 0 \qquad (4)$$

3. RESULTS AND DISCUSSION

At Fig. 5 the main flux dependence on the input voltage $\Psi_{mV}=f(U)$ (in relative units of the nominal input voltage U_n) of the voltage transformation core at constant input current I of the current transformation core is given. At Fig. 6 the main flux dependence on the input current $\Psi_{mC}=f(U)$ (in relative units of the nominal input current I_n) of the current transformation core at constant input voltage U of the voltage transformation core is shown. The leakage fluxes in the air as well as the electromagnetic influence between the two magnetic measuring cores are calculated, also. After the magnetic field distribution in different parts of the combined instrument transformer is numerically calculated the main parameters of the transformer are estimated as the leakage

reactances of the windings (primary and secondary) for different loads (input currents and voltages).

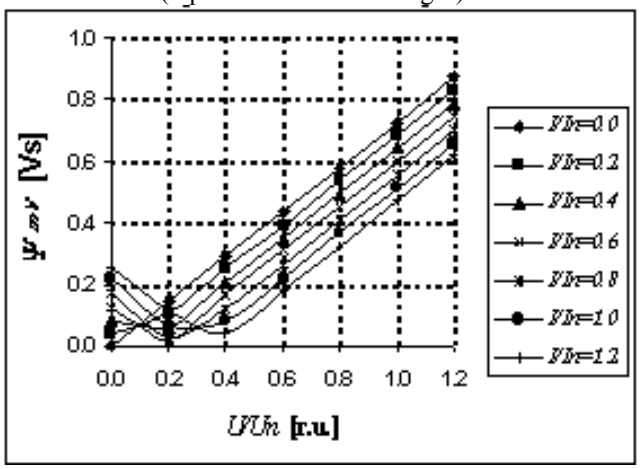

Fig. 5. Numerically calculated main flux in the voltage transformation core Ψ_{mV}

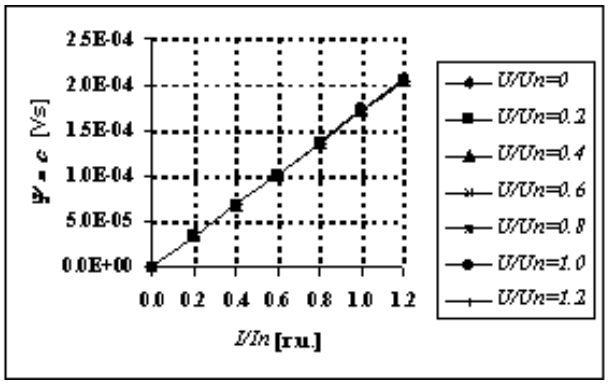

Fig. 6. Numerically calculated main flux in the current transformation core Ψ_{mC}

The numerically calculated leakage reactances of the primary voltage winding $X_{\sigma v1}$ are given in Table 1., of the secondary voltage winding $X_{\sigma v2}$ in Table 2., of the primary current winding $X_{\sigma c1}$ in Table 3., and of the secondary current winding $X_{\sigma c2}$ in Table 4. In all tables the U/U_n ratio is the relative value of the input voltage of the voltage transformation core to its nominal value and the I/I_n ratio is the relative value of the input current of the current transformation core to its nominal value. This enables exact calculation of the voltage p_u, current p_i, and phase difference errors δ_u and δ_i of the two measurement cores. At Fig. 7. and Fig. 8. the families of numerically calculated characteristics of the relative voltage and phase difference errors depending on the input voltage of the voltage transformation core at constant input currents of the current transformation core are displayed. At Fig. 9. and Fig. 10. the families of numerically calculated characteristics of the relative current and phase difference errors depending on the input current of the current transformation core at constant input voltages of the voltage transformation core are displayed. The electromagnetic influence of the current load of the current transformation core on the flux distribution in the voltage transformation core can be seen from the family of flux characteristics in Fig. 5. This leads to changes of the error characteristics, shown in Fig. 7 and Fig. 8. Especially for the lower values of the input voltage of the voltage transformation core. The electromagnetic influence of the current transformation core decreases as the input voltage increases. The accuracy class of the voltage transformation core with the electromagnetic influence of the current transformation core is 3.

TABLE 1. Leakage reactances of the primary winding of the voltage transformation core

I/In	**0,0**	**0,2**	**0,4**	**0,6**	**0.8**	**1,0**	**1,2**
U/Un	$X_{\sigma v1}$ **MΩ**	$X_{\sigma v1}$ **MΩ**	$X_{\sigma v1}$ **MΩ**	$X_{\sigma v1}$ **MΩ**	$X_{\sigma v1}$ **MΩ**	$X_{\sigma v1}$ **MΩ**	$X_{\sigma v1}$ **MΩ**
0,2	525	481	400	336	271	208	146
0,4	530	499	467	435	402	371	340
0,6	526	505	483	462	441	419	399
0,8	527	511	495	479	463	447	432
1,0	528	515	508	489	477	464	452
1,2	529	518	508	497	486	475	465

TABLE 2. Leakage reactances of the secondary winding of the voltage transformation core

I/In	**0,0**	**0,2**	**0,4**	**0,6**	**0,8**	**1,0**	**1,2**
U/Un	$X_{\sigma v2}$ **Ω**	$X_{\sigma v2}$ **Ω**	$X_{\sigma v2}$ **Ω**	$X_{\sigma v2}$ **Ω**	$X_{\sigma v2}$ **Ω**	$X_{\sigma v2}$ **Ω**	$X_{\sigma v2}$ **Ω**
0,2	0,91	0,83	0,69	0,58	0,47	0,36	0,25
0,4	0,92	0,87	0,81	0,75	0,70	0,64	0,59
0,6	0,91	0,88	0,84	0,80	0,76	0,73	0,69
0,8	0,91	0,89	0,86	0,83	0,80	0,78	0,75
1,0	0,92	0,89	0,88	0,85	0,83	0,80	0,78
1,2	0,92	0,90	0,88	0,86	0,84	0,82	0,81

TABLE 3. Leakage reactances of the primary winding of the current transformation core

U/Un	**0,0**	**0,2**	**0,4**	**0,6**	**0,8**	**1,0**	**1,2**
I/In	$X_{\sigma c1}$ **μΩ**	$X_{\sigma c1}$ **μΩ**	$X_{\sigma c1}$ **μΩ**	$X_{\sigma c1}$ **μΩ**	$X_{\sigma c1}$ **μΩ**	$X_{\sigma c1}$ **μΩ**	$X_{\sigma c1}$ **μΩ**
0,2	998	988	979	968	960	949	942
0,4	999	994	990	984	979	975	970
0,6	999	995	992	989	986	982	979
0,8	999	997	994	992	989	987	985
1,0	998	996	995	992	990	989	987
1,2	995	993	992	990	988	987	985

TABLE 4. Leakage reactances of the secondary winding of the current transformation core

U/Un	**0,0**	**0,2**	**0,4**	**0,6**	**0,8**	**1,0**	**1,2**
I/In	$X_{\sigma c2}$ **mΩ**	$X_{\sigma c2}$ **mΩ**	$X_{\sigma c2}$ **mΩ**	$X_{\sigma c2}$ **mΩ**	$X_{\sigma c2}$ **mΩ**	$X_{\sigma c2}$ **mΩ**	$X_{\sigma c2}$ **mΩ**
0,2	127	125	124	123	122	121	120
0,4	127	126	126	125	124	124	123
0,6	127	126	126	126	125	125	124
0,8	127	127	126	126	126	125	125
1,0	127	126	126	126	126	125	125
1,2	126	126	126	126	125	125	125

The electromagnetic influence of the voltage transformation core to the magnetic field distribution in the current transformation core is negligible as in Fig. 6.

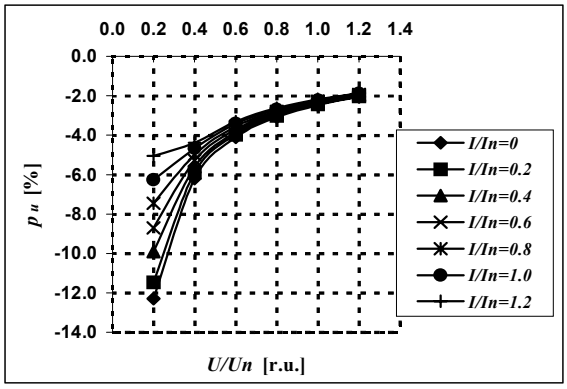

Fig. 7. Relative voltage error dependencies on the input voltage of the voltage transformation core

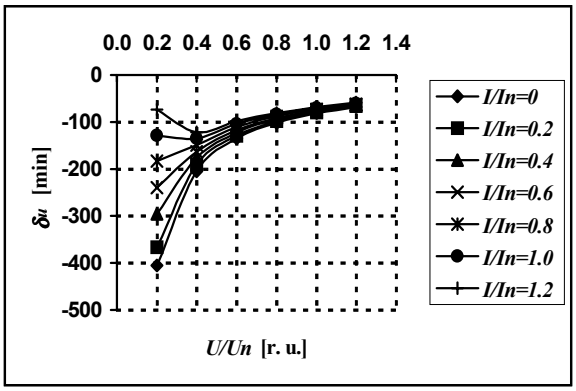

Fig. 8. Phase difference error dependencies on the input voltage of the voltage transformation core

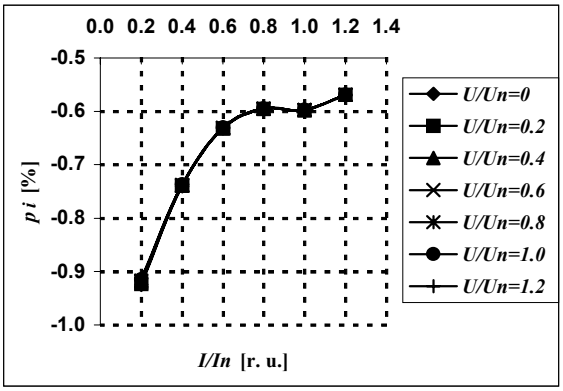

Fig. 9. Relative current error dependencies on the input current of the current transformation core

Therefore variation of the error characteristics of the current transformation core are very low as the input voltage of the voltage transformation core varies as displayed at Fig. 9. and 10. The accuracy class of the current transformation core with the electromagnetic influence of the voltage transformation core is 1.

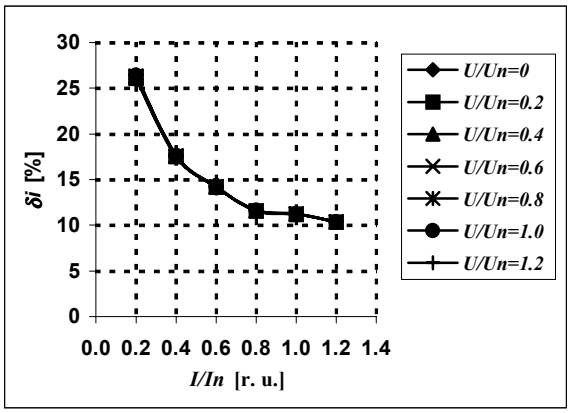

Fig. 10. Phase difference error dependencies on the input current of the current transformation core

4. CONCLUSIONS

In the paper an original calculation of the magnetic field distribution in the three-dimensional domain of the combined current-voltage instrument transformer is made. The FEM-3D calculated voltage, current and phase difference errors of the combined current-voltage instrument transformer enable exact estimation of the winding correction factors for achieving higher metrological accuracy of the instrument transformer. This methodology allows further optimal design of the instrument transformer and improvement of its metrological parameters and achievement of higher accuracy class by taking into account the mutual electromagnetic influence of the both magnetic cores of the transformer.

REFERENCES

[1] IEC 60044-3 (1980-01): Instrument Transformers, Part 3: Combined Transformers, 1980.

[2] V. Bego, "Mjerni transformatori", *Skolska knjiga,* Zagreb, 1977.

[3] E. Lesniewska, J. Chojancki "Influence of the Correlated Localisation of Cores and Windings on Measurement Properties of Current Transformers", *Proc. of 10th Int. Symposium on Electromagnetic Fields in Electrical Engineering ISEF 2001* pp. 281-286, Cracow, Poland, 2001.

[4] E. Lesniewska, "Influence of External Fields and Constructional Elements on Leakage Field Distribution of Current Transformer", *Proc. of 18th Int. Workshop Advanced Simulation Systems ACTA MOSIS* No. 62 pp. 61-66, Ostrava, Czech R., 1996.

[5] M. Cundev, L. Petkovska, V. Stoilkov "3D Magnetic Field Calculation in Compound Configurations", *Proc. of Int. Conf on Advanced Computational Methods in Engineering ACOMEN'98,* pp. 503-510, Ghent, Belgium, 1998.

[6] G. Ramm, G. Roeissle, H. G. Latzel "Computer Controlled Calibration Measurement System for Current and Voltage Instrument Transformers" ("Rechnergesteuerte Kalibrierung von Messeinrichtingen fuer Strom- und Spannungswandler"), *PTB-Mitteilungen*, No. 108 vol. 3/98, pp. 188-200, Braunschweig, Germany 1998.

Authors:

Marija Cundeva, MSc, University "Sts. Cyril&Methodius", Faculty of Electrical Engineering, Karpos II, b.b. POBox 574, 1000 Skopje, R. Macedonia , Phone: +398 2 399162, Fax: +389 2 364262, E-mail: mcundeva@cerera.etf.ukim.edu. mk

Ljupco Arsov, Ph.D, Prof., University "Sts. Cyril&Methodius", Faculty of Electrical Engineering, Karpos II, b.b. POBox 574, 1000 Skopje, R. Macedonia , Phone: +398 2 399111, Fax: +389 2 364262, E-mail: ljarsov@cerera.etf.ukim.edu. mk